JOURNAL OF GEOPHYSICAL RESEARCH, VOL. 113, A08214, doi:10.1029/2007JA012896, 2008

Short-burst auroral radiations in Alfvénic acceleration regions: FAST observations

Yi-Jiun Su,[1] Lun Ma,[1] Robert E. Ergun,[2] Philip L. Pritchett,[3] and Charles W. Carlson[4]

Received 19 October 2007; revised 15 February 2008; accepted 9 April 2008; published 12 August 2008.

[1] We examined particle and field data during the first 3 years (1997–1999) of the FAST mission searching for short-burst auroral kilometric radio (AKR) emissions in Alfvénic auroral acceleration regions. Eight such events were found at altitudes between 2500 and 3600 km in the midnight local time sector during winter months when the AE index was observed to be greater than 150. The emission source regions are estimated to be ~300–900 km below the satellite. The frequency of observed short-bursts is in the range between 400 and 600 kHz. The average bandwidth of the burst, $\Delta f/f$, is approximately 2×10^{-2}. The reoccurrence frequency of discrete short bursts is estimated to be between 7 and 18 Hz, which is similar to that of Jovian S-bursts. The negative drift of each discrete burst may be associated with upward moving electrons. As in the case for ordinary AKR, short-bursts can be explained by the electron cyclotron maser instability due to the positive gradient in the phase space of an unstable electron distribution. Shell, conic, and ring distributions, and a combination of these three, were observed in each of the eight events. Snapshots of observed multiple shells and rings are suggested to be the results of the temporal effect, where low energy electrons are accelerated by the Alfvénic perturbation at an earlier time, while high energy electrons are newly accelerated by later Alfvénic pulses. Results presented within this paper suggest multiple Alfvénic disturbances in the magnetotail as the source of the multiple shell (and ring) distributions. Multiple Alfvénic disturbances may also explain the observed reoccurrence pattern of short-bursts.

Citation: Su, Y.-J., L. Ma, R. E. Ergun, P. L. Pritchett, and C. W. Carlson (2008), Short-burst auroral radiations in Alfvénic acceleration regions: FAST observations, *J. Geophys. Res.*, *113*, A08214, doi:10.1029/2007JA012896.

1. Introduction

[2] The first satellite that carried radio receivers made the surprising discovery that the Earth is an intense radio source [*Benediktov et al.*, 1965]. These radio emissions are referred to as Auroral Kilometric Radiation (AKR), because they are observed to peak at ~200–500 kHz and are generated at altitudes between 2000 and 10,000 km above the auroral region in association with visible auroral arcs [e.g., *Gurnett*, 1974]. Similar auroral emissions have also been observed from all magnetized planets in our solar system [e.g., *Zarka*, 1992, 1998].

[3] AKR originates on auroral field lines where downgoing ''inverted-V'' electrons are accelerated [e.g., *Gurnett*, 1974; *Kurth et al.*, 1975; *Benson and Calvert*, 1979]. Radio wave and ray tracing analysis indicate that AKR is generated in regions of depleted plasma density near the local electron cyclotron frequency [*Hilgers*, 1992]; hence it is assumed that the waves are generated from the free energy of non-Maxwellian auroral electron distributions. These waves propagate primarily in the R-X mode [e.g., *Gurnett and Green*, 1978; *Kaiser et al.*, 1978; *Benson and Calvert*, 1979; *Shawhan and Gurnett*, 1982] and show strong temporal variations and fine spectral features [e.g., *Gurnett et al.*, 1979; *Menietti et al.*, 2000].

[4] Fine structures of AKR have been reported since the late 1970s. *Gurnett et al.* [1979] using ISEE data, and *Gurnett and Anderson* [1981] and *Benson et al.* [1988] using DE 1 data, and *Morioka et al.* [1981] using Exos-B data reported AKR fine structures in both the ordinary and extraordinary modes. They showed that observed frequency drift rates of fine structures are in the range of 100 Hz/s–10 s kHz/s. From data obtained by the Polar/plasma wave instrument, *Menietti et al.* [2000] showed that AKR patterns with very narrow-band, negative drifting stripes (40–215 kHz) occur in ~6.6% of the fine structure data. Often fainter than the background AKR spectrum, the stripes are most easily identified extending below the frequency band of the more diffuse AKR spectral features. The negative-sloped stripes have a frequency extent of about 4 kHz and a typical time duration of less than 2 s. The upper limit on the frequency bandwidth of an individual stripe is at $\Delta f/f \sim 4 \times 10^{-3}$.

[1]Physics Department, University of Texas at Arlington, Arlington, Texas, USA.
[2]Laboratory for Atmospheric and Space Physics, University of Colorado, Boulder, Colorado, USA.
[3]Department of Physics and Astronomy, University of California, Los Angeles, California, USA.
[4]Space Sciences Laboratory, University of California, Berkeley, California, USA.

0148-0227/08/2007JA012896$09.00

Recently, *Ergun et al.* [2006] and *Su et al.* [2007] reported an example of possible Earth-based short bursts detected by the FAST satellite at the polar cap boundary during a substorm expansion. These short-burst emissions at Earth are analogous to S-bursts remotely observed from Jupiter. Since the discovery of Jovian S-bursts [*Kraus*, 1956; *Gallet*, 1961], numerous reports on the morphology and characteristics have been published in literature [e.g., *Baart et al.*, 1966; *Riihimaa*, 1977; *Desch et al.*, 1978; *Ellis*, 1980; *Leblanc et al.*, 1980; *Carr et al.*, 1983; *Genova and Calvert*, 1988; *Dulk et al.*, 1992; *Zarka et al.*, 1996; *Carr and Reyes*, 1999; *Queinnee and Zarka*, 2001; *Ryabov et al.*, 2007].

[5] Several physical mechanisms have been proposed to explain the observed fine structures of the planetary radio emissions. *Lecacheux et al.* [1981] indicated that various propagation effects, such as refraction, diffraction, and focusing, due to plasma inhomogeneities can account for some of fine structures of the planetary radio emissions. *Melrose* [1986] proposed a feedback model that depends on a phase-bunching mechanism. *Calvert et al.* [1988] proposed that the natural "radio lasing" might explain the S-burst frequency drift. *Winglee et al.* [1988] and *Pritchett and Winglee* [1989] showed that the maser emission tends to be produced in the form of discrete wave packets. *Carr and Reyes* [1999] explained that the Jovian S-bursts are due to the upward moving electrons. *Winglee et al.* [1992] suggested that the bursty emissions are associated with impulsive injection in which the electron distribution can develop a beam feature with temperature anisotropy. The temperature anisotropic beam instability would then convert particle energy into electromagnetic energy with similar efficiency as the maser instability; however, this emission is larger than the local cyclotron frequency. *Menietti et al.* [1996, 1997] suggested that the negative-slope striated bursts are produced by stimulation of the source region by electromagnetic ion cyclotron waves traveling away from Earth. Although several suggestions of the source mechanism have been proposed, the interpretation of the fine structure is still largely open to conjecture [*Louarn*, 1992]. Radio bursts constitute one of the major remaining puzzles in the physics of planetary radio emissions [*Zarka*, 2004].

[6] To date, the most successful explanation proposed for the generation of AKR is the electron cyclotron maser [e.g., *Wu and Lee*, 1979; *Melrose and Dulk*, 1982; *Hewitt et al.*, 1982], in which radiation excited near the local electron cyclotron frequency is amplified through a gyroresonant interaction [*Melrose and Dulk*, 1982]. The same mechanism is also believed to power decametric radio emissions (DAM) [e.g., *Melrose*, 1976; *Hewitt et al.*, 1981], as well as analogous radiation from the other magnetized outer planets [e.g., *Zarka*, 1992]. The generation mechanism of the cyclotron maser was established originally based on observed loss cone electrons where a nonequilibrium distribution with the free energy stored in the transverse velocity derivative $\partial f_e/\partial v_\perp > 0$ of the electron distribution function [e.g., *Wu and Lee*, 1979; *Melrose and Dulk*, 1982]. The electrons forming the gradient at the loss cone boundary shed their excess perpendicular energy, excite electromagnetic waves, and fill the loss cone until the gradient is diminished. On the basis of studies of Viking and FAST observations [*Louarn et al.*, 1990; *Delory et al.*, 1998; *Ergun et al.*, 1998, 2000; *Strangeway et al.*, 1998] and numerical simulations [e.g., *Pritchett et al.*, 1999, 2002], a modification of the cyclotron maser mechanism that is now accepted in the space science community is that an unstable shell (horseshoe) electron distribution produced by quasi-static parallel electric fields in the density cavity of the upward current region is able to provide sufficient free energy to power AKR.

[7] From the comparison between the simulation results [*Su et al.*, 2007] and FAST data [*Ergun et al.*, 2006], the authors recently suggested that unstable shell distribution functions may be generated by parallel electric fields associated with inertial Alfvén waves in a dynamic Alfvénic acceleration region. In addition, electrons outside the loss cone are reflected back up the flux tube due to the mirror force, forming a conic (or ring) signature in the 2D (3D) phase space, which is also an unstable distribution. This paper presents results based on a systematic study of short burst observations in the Alfvénic acceleration region that expands upon the single event study by *Ergun et al.* [2006] and *Su et al.* [2007].

2. Data Selection Criteria

[8] The results presented in this paper are based on data obtained from the FAST satellite during the first 3 years in orbit (1997–1999) when the electric field instrument was fully operational. With approximately ten thousand orbits during this period, it was necessary for us to define criteria for selecting events of interest. As the study progressed, the process of event identification evolved based on our experiences.

[9] 1. Auroral Electrojet (AE) $\geq$ 150. *Ergun et al.* [2006] showed that short-bursts are observed during the recovery phase of the substorm. In general, substorms are associated with high AE indices, hence, we selected the date and time when AE was greater than 150. Values for the AE index used in this study were obtained from a website provided by the World Data Center for Geomagnetism in Kyoto. It should be noted that we also occasionally examined data during periods when AE < 150. The Alfvénic acceleration event occurs infrequently during those periods.

[10] 2. Enhanced counterstreaming electrons. Because we are interested in short-burst observations in the Alfvénic acceleration region, we first identified the periods where electron accelerations was dominated by Alfvén waves. Enhanced counterstreaming electrons are associated with Alfvénic perturbations in the auroral regions [*Su et al.*, 2001; *Chaston et al.*, 2002a, 2002b; *Lysak and Song*, 2003]; hence, we utilized this distinct characteristic to select possible candidates from summary plots on the official FAST website provided by the University of California at Berkeley.

[11] 3. FAST orbits with high-resolution data. The instruments on the FAST satellite operate in two modes: the survey mode and the burst mode. Typically, the burst data span 10–30 s and allow the detailed investigation of small-structures in auroral acceleration regions such as fine structures of AKRs recorded by the on-board Plasma Wave Tracker (PWT) [*Ergun et al.*, 2001]. Since our study focuses on these fine scale structures, we only selected orbits containing high time resolution data and eliminated data in the survey mode.

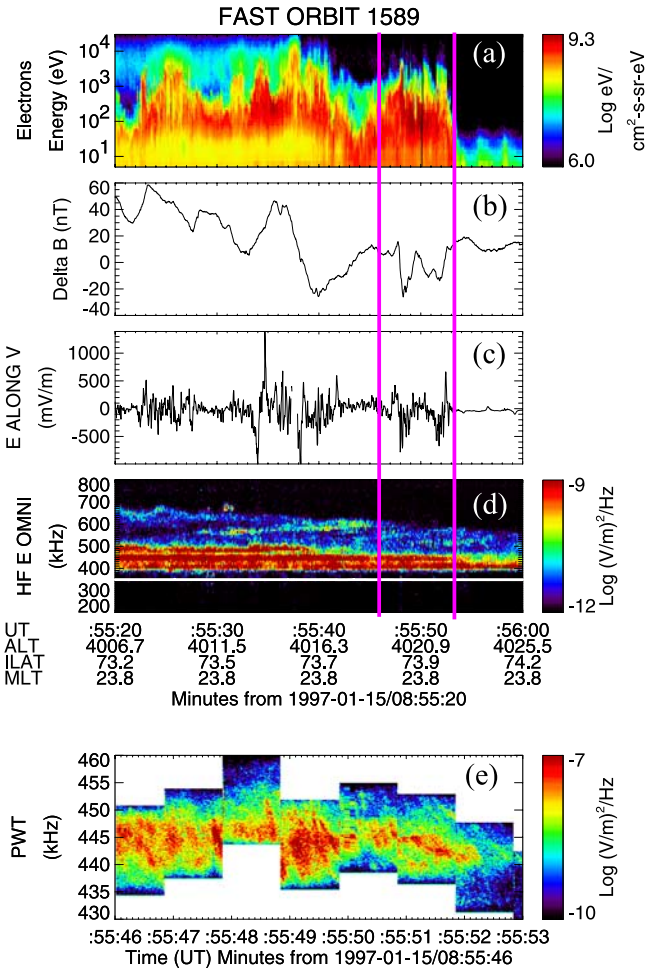

Figure 1. FAST orbit 1589 at 0855:20–56:00 UT on 15 January 1997. (a) The electron energy-time spectrogram. (b) The magnetic field perturbation perpendicular to the direction of the satellite trajectory. (c) The electric field along the spacecraft trajectory. (d) The electric field spectral power density where the white line indicates the local electron cyclotron frequency. (e) An expanded view of the electric field spectral power density from PWT at 0855:46–53 UT.

[12] 4. Coexistence of Alfvén waves and AKR emissions. Alfvénic perturbations are often observed in the polar cap boundary region which includes the dayside cusp [e.g., *Su et al.*, 2001] and near the midnight polar cap boundary [*Wygant et al.*, 2000; *Keiling et al.*, 2001, 2003]. Several distinct features in the polar cap boundary acceleration region are summarized here: (1) highly variable current, which can be temporally or spatially averaged to little net current; (2) The ratio of electric field and magnetic field perturbations on the order of 10^4 km/s similar to the local Alfvén speed; (3) enhanced energy fluxes of field-aligned electrons; and (4) enhanced energy fluxes of ion conics. We examined FAST field and particle data to select Alfvénic acceleration events with the features described above. On the basis of our initial search, we found 186 orbits with Alfvénic signatures out of 2290 FAST orbits from 1 January to 1 August 1997, which corresponds to an occurrence rate of ~8%.

[13] We then examined the electric field power density spectrum from the Swept Frequency Analyzer (SFA) [*Ergun et al.*, 2001] to identify AKR emissions from Alfvénic acceleration events. We selected events for further analyses only when AKR emissions and Alfvénic acceleration signatures were simultaneously observed.

[14] 5. Identify discrete short-burst emissions through examination of high time resolution PWT data. AKR emissions are obtained in both the survey and burst modes of SFA. For fine structure measurements such as short-bursts, it is necessary to examine the high time resolution power spectra density obtained from PWT [*Ergun et al.*, 2001]. Our final step is to select specific events when discrete short-bursts with time-of-flight dispersion signatures can be easily identified.

3. Observational Results

[15] Based on the selection criteria described in the previous section, eight events were identified during the first 3 years of the FAST mission where short-burst emissions were simultaneously observed with Alfvénic acceleration signatures including the case (orbit 1906) previously reported by *Ergun et al.* [2006] and *Su et al.* [2007]. A typical example of such event is plotted in Figure 1. Short-burst emissions are presented in Figure 1e which is an expanded view between the two vertical magenta lines in Figure 1d. The ratio of the electric field (Figure 1c) and magnetic field (Figure 1b) between the two magenta lines corresponds to a wave speed of 10^4 km/s, consistent with the local Alfvén speed.

[16] Eight short-burst events are listed in Table 1, where the first, second, and the third columns are the FAST orbit number, date, and the universal time/magnetic local time, respectively. The peak *AE* index within 3 h of each observation is listed in the fourth column of Table 1. f, f_{re}, and f_{ce} represent the wave frequency range, and the reoccurrence rate of discrete short-bursts and the local electron cyclotron frequency, respectively. The local electron cyclotron frequency is obtained from $f_{ce} = eB/m_e$, where B, e, and m_e are the total magnetic field obtained from the DC magnetometer, and the electron charge and mass. The average bandwidth of short-bursts ($\Delta f/f$) is estimated to be $\sim 2 \times 10^{-2}$. By assuming a simple dipole magnetic field ($B \propto 1/r^3$), the distance to the emission source region is estimated as $r_{source} = r_{sat}(f_{ce}/f_{Sburst})^{1/3}$, where r_{sat} is the satellite's location in geocentric distance (assuming 1 R_E = 6378 km), and f_{Sburst} is the short-burst frequency obtained by PWT. We note that f_{Sburst} is assumed to be the electron cyclotron frequency at the source region. In Table 1, D_{sat}, D_{source}, and (D_{sat}–D_{source}) represent the satellite's location above the Earth's surface, the estimated source location of the emissions, and the distance between the source region and the satellite, respectively. The electric field spectral power densities from each of the eight events are plotted in Figure 2.

[17] The characteristics of short burst events in the Alfvénic acceleration regions are discussed below.

[18] 1. All of the eight events occurred on the nightside, specifically between 21:00 and 1:00 magnetic local time (MLT, see the third column of Table 1). Although a few cases were found with kilometric emissions in the dayside

Table 1. A List of Eight Short-Burst Events

Orbit	Date	UT/MLT	*AE*	*f* kHz	f_{re} Hz	f_{ce} kHz	D_{sat} km	D_{source} km	D_{sat}-D_{source}	f_{pe}/f_{ce}
1504	01–07–97	12:14/0.4	750	473–482	7–9	367	3827	2940–3000	827–887	0.49
1589	01–15–97	08:55/23.8	250	437–452	8–10	348	4020	3152–3260	760–868	0.26
1845	02–08–97	01:17/22.9	400	457–466	10–17	350	3914	2977–3038	876–937	0.36
1906	02–13–97	16:49/22.8	250	558–570	10–18	455	3217	2523–2586	631–694	0.28
1915	02–14–97	12:46/21.3	300	515–525	8–10	435	3334	2744–2803	531–590	0.29
1940	02–16–97	20:13/22.7	500	465–470	8–10	415	3350	2955–2988	362–395	0.31
1952	02–17–97	22:49/22.3	450	500–513	8–10	398	3432	2636–2714	718–796	0.39
6903	05–21–98	11:08/0.8	510	398–407	9–10	339	4143	3521–3595	548–622	0.15

auroral region, they were not selected for analysis because the signals were too weak. The nightside polar cap boundary acceleration region (i.e., Alfvénic acceleration region) is often observed near midnight which maps to the magnetotail reconnection region.

[19] 2. All identified events occurred during winter months. Two events were observed in January and five in February. The majority of events were obtained in the Northern Hemisphere, while one event (orbit 6903) was observed in the Southern Hemisphere in May 1998. On the basis of a 7-year survey of the occurrence of AKR events, *Kumamoto and Oya* [1998] found that AKR is more common in the winter hemisphere than in the summer hemisphere. We found that the short-burst AKR also follows the same behavior.

[20] 3. A negative frequency drift is observed for each observed discrete burst. This phenomenon indicates that the source altitude increases with decreasing local electron

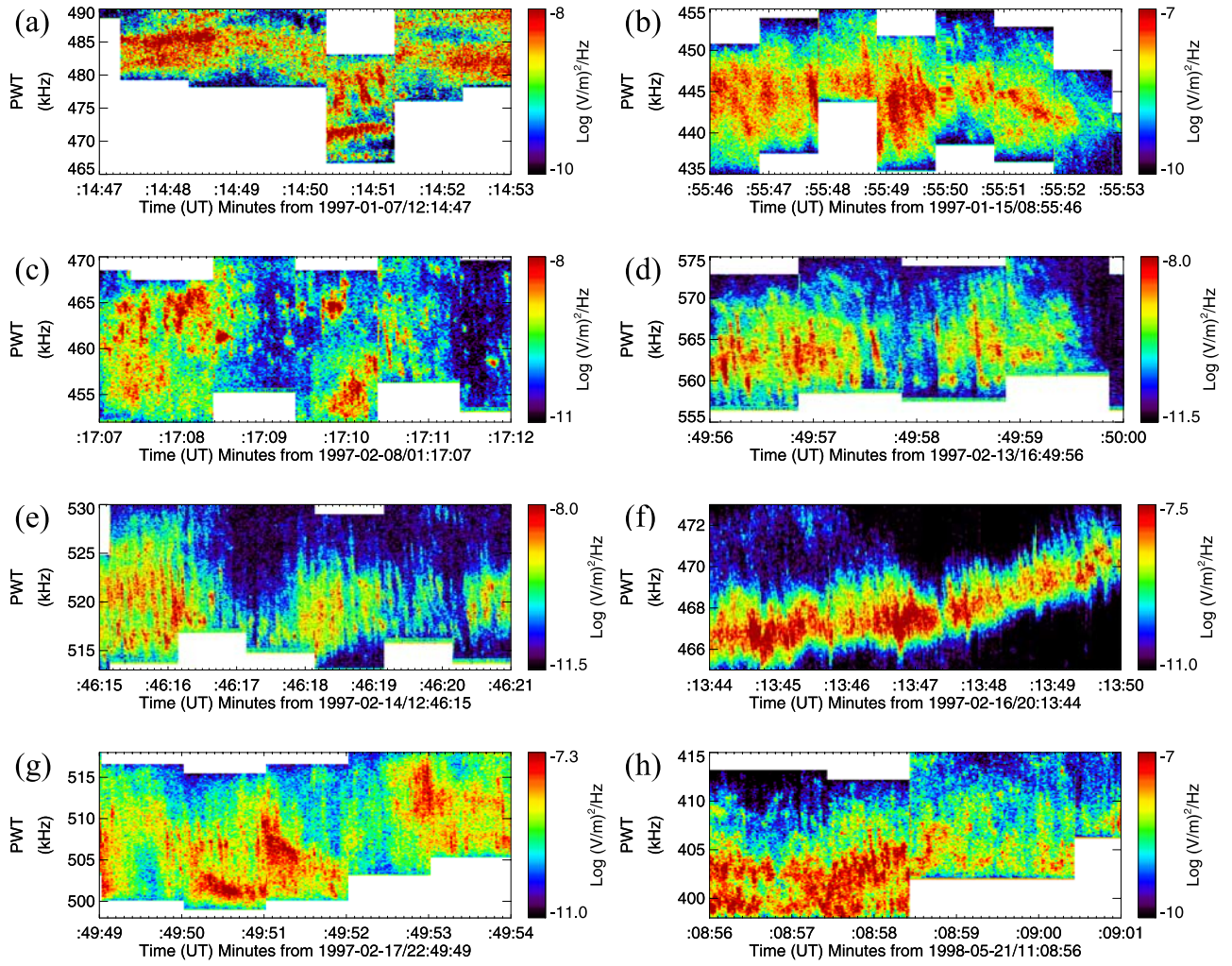

Figure 2. Short-burst emissions observed from the FAST satellite. (a) Orbit 1504 at 1214:47–53 UT on 7 January 1997. (b) Orbit 1589 at 0855:46–53 UT on 15 January 1997. (c) Orbit 1854 at 0117:07–12 UT on 8 February 1997. (d) Orbit 1906 at 1649:56–50:00 UT on 13 February 1997. (e) Orbit 1915 at 1246:15–21 UT on 14 February 1997. (f) Orbit 1940 at 2013:44–50 UT on 16 February 1997. (g) Orbit 1952 at 2249:49–54 UT on 17 February 1997. (h) Orbit 6903 at 1108:56–09:02 UT on 21 May 1998.

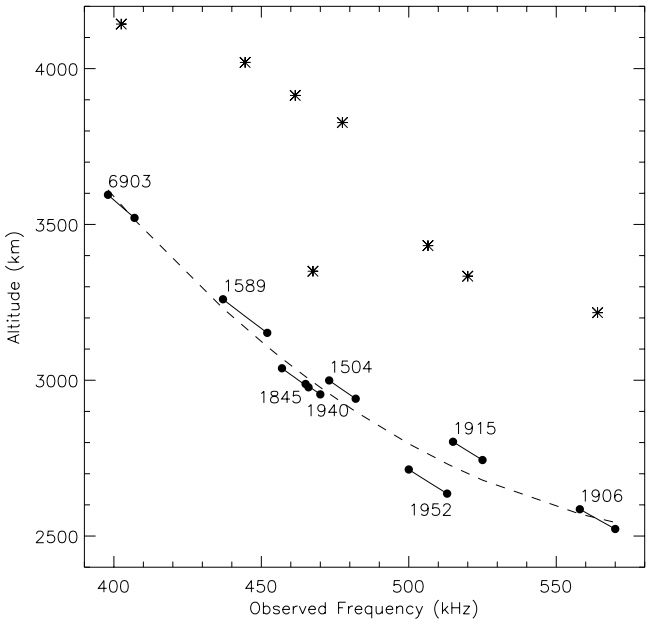

Figure 3. Estimated emission source location versus the observed short-burst frequency based on eight events. The dashed line represented a polynomial fit with a degree of three. Asterisks are used to represent the satellite locations.

cyclotron frequency (i.e., decreasing magnetic field). The negative drift may be associated with upward moving electrons. As is the case for ordinary AKR, short-burst emissions can be explained by the electron cyclotron maser instability due to the positive gradient in the phase space of an unstable electron distribution. The frequencies of short-bursts lie within a range between 398 and 570 kHz as listed in the fifth column of Table 1.

[21] 4. The average duration of a single burst is ~0.1 s. The reoccurrence rate of short bursts ranges between 7 and 18 Hz (see the sixth column of Table 1), which is similar to the reoccurrence rate of Jovian S-bursts. *Su et al.* [2006] suggested the ionospheric Alfvén resonator as a likely driver explaining the multiple occurrences of S-bursts because they showed that the fundamental frequency and higher harmonics of the Alfvén resonator are comparable to the observed reoccurring frequency of S-bursts based on results of 1D linear gyrofluid simulations. The reoccurrence rate of short-bursts observed by FAST is one order of magnitude higher than the typical frequency (~1 Hz) of Earth's ionospheric Alfvén resonator [*Lysak*, 1993].

[22] 5. The source regions of short-bursts are located between 2500 and 3600 km above the Earth's surface and below the satellite (see the 8th-10th columns in Table 1). The apogee of FAST is near 4200 km, hence, no observation was made above this altitude. No event was found at low altitudes near the perigee (~315 km) of FAST. The shortest distance between the source region and the satellite is ~360 km. Although we did not find cases in which short bursts occurred above the satellite, this does not exclude the possibility of a higher source region. Since no event was found where the satellite passed directly through the emission source region, we are not able to determine the plasma conditions of the source. However, the ratios of plasma frequency and electron cyclotron frequency at observational points are listed in the last column of Table 1.

[23] The estimated emission source altitude (the 9th column of Table 1) versus the observed frequency (the fifth column of Table 1) of all eight events is plotted in Figure 3, where asterisks denote the satellite location (the eighth column of Table 1) for each case. The emission is assumed to be generated locally due to unstable electron distributions; hence, the emission frequency on the x axis represents the electron cyclotron frequency in the source region. The dashed line represents the polynomial fit with the degree of three. A negative slope in Figure 3 indicates a converging dipole magnetic field model assumed in our study. The offset of the data points from the dashed line could indicate the variation of emission source latitudes or might be due to the dynamics of the Earth's magnetic field.

[24] 6. The spectral power density of short bursts is one or two orders of magnitudes weaker than that of common AKR emissions. The peak electric field spectral power density of typical AKR emissions observed from the FAST satellite is on the order of 10^{-6} $(V/m)^2/Hz$ (not shown here), while the peak power density of short-bursts is $\sim 10^{-8}$–10^{-7} (V/m)2/Hz. If short-bursts and AKRs are present simultaneously, it would be difficult to distinguish weak short-burst emissions from strong AKR signals. Hence eight events from 3 years of data represent the minimum occurrence rate when short-bursts were observed in Alfvénic auroral acceleration regions.

[25] 7. Observed unstable electron distributions are associated with short-burst emissions. Single shell, multiple shells, and ring (or conic) distributions were observed in each of the eight short-burst events. Selected electron distributions associated with short-bursts in the Alfvénic auroral acceleration region are displayed in Figure 4, where the horizontal and vertical axes are the parallel and perpendicular velocities and the negative x is in the direction away from the Earth's ionosphere. These electrons distributions were selected from three of the eight events to demonstrate the common features. We did not include all electron distributions in this paper due to the similarity of their features. Single and multiple shell distributions are shown in Figures 4a–4c. We should note that many shell (horseshoe) distributions did not have full coverage in the angular bins outside of the loss cone. An example of a partial shell distribution can be seen in the downward direction ($+x$) in Figure 4g.

[26] According to the simulation work by *Su et al.* [2007], Alfvénic perturbations can be generated by multiple pulses at high altitudes. Assuming a stationary observational point as the satellite, the inner shell (i.e., lower energy electrons) in the phase space distribution is generated by the perturbation pulse arriving first, while the outer shells (i.e., higher energy electrons) are due to perturbations which reach the satellite at later times. Hence we interpret the observed snapshot of multiple shells as the result of temporal variation. *Su et al.* [2007] showed that electrons outside the loss cone are reflected back up the flux tube due to the mirror force, forming a conic (ring) signature in the 2D (3D) phase space. An example of a ring distribution is shown in Figure 4d, while an electron conic is displayed in

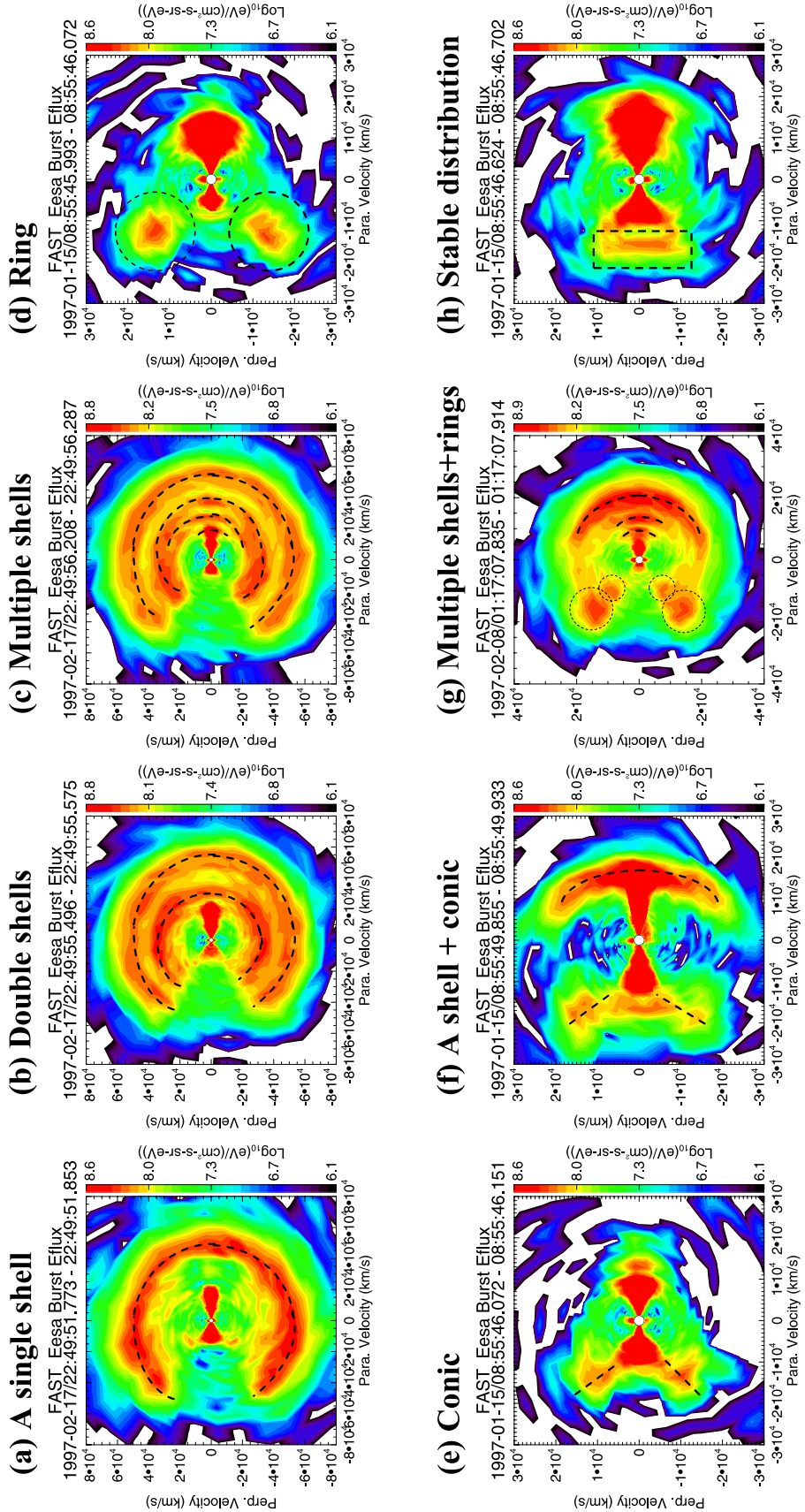

Figure 4. Electron distributions observed in the Alfvénic acceleration region by the FAST satellite during short-burst events. The time resolution of each distribution is 79 ms. The horizontal and vertical axes represent the parallel and perpendicular velocities, respectively, where the upward direction away from the Earth's ionosphere is to the left. The differential energy flux is represented by the color according to the color bar on the right. (a) A single shell distribution at 2249:51.77 UT, (b) a double shell at 2249:55.50 UT, and (c) a multiple shell distribution at 2249:56.21 UT on 17 February 1997. (d) A ring distribution at 855:45.99 UT, (e) a conic distribution at 0855:46.07 UT, and (f) shell and conic distributions at 0855:49.86 UT on 15 January 2007. (g) Multiple shells and rings at 0117:07.84 UT on 8 February 1997. (h) A stable distribution may have resulted from an unstable ring at 0855:46.62 UT on 15 January 1997. The dashed lines indicate the important feature for each distribution.

Figure 4e. The combination of the conics (or rings) and partial shell(s) is demonstrated in Figures 4f and 4g. This type of distributions is thought to be due to the temporal effect where rings are generated by mirrored electrons caused by Alfvén pulses arriving earlier and shells are due to later pulses.

4. Discussion and Summary

[27] In this study, we examined FAST data during the first 3 years (1997–1999) of operation. Eight events were found when short-bursts were observed simultaneously with Alfvénic accelerated electrons in the polar cap boundary region based on the criteria described in section 2. Each of these events was found in the midnight sector during winter months within an altitude range of 2500–3600 km. The ionospheric density decreases with increasing altitudes, hence, these cases found near the higher altitude range of the FAST orbit suggest that short-burst events prefer low plasma density conditions. Because the dayside ionosphere receives direct sunlight, the ionization rate at night is lower than that on the dayside. Moreover, the ionization rate is lower during winter than in summer. The preferred occurrence on the nightside and during winter suggests a preference for low plasma density conditions.

[28] In order for the weakly relativistic cyclotron maser instability to occur, one important condition is a very low background plasma density meaning that the ratio of plasma frequency and electron cyclotron frequency should be much less than one, i.e., $\omega_{pe}/\omega_{ce} \ll 1$ [e.g., *Ergun et al.*, 2000; *Pritchett et al.*, 2002]. The ratio of local ω_{pe}/ω_{ce} value ranges from 0.15 to 0.5 (the last column of Table 1) based on eight events, which is one order of magnitude higher than that for the intense AKR events described by *Pritchett et al.* [2002]. Although the local plasma frequency is less than the cyclotron frequency at observed altitudes, it might still not meet the requirement of the maser instability. Since no event was found when the satellite passed directly through the emission source region, we were not able to determine the exact quantity of ω_{pe}/ω_{ce} in order to trigger the short burst radiations.

[29] The reoccurrence frequency of discrete short bursts is estimated to be between 7 and 18 Hz similar to Jovian S-bursts. *Su et al.* [2006] and *Ergun et al.* [2006] suggested the ionospheric Alfvén resonator as a likely driver explaining multiple occurrences of short-bursts. Although the reoccurrence frequency of discrete short bursts observed from FAST is one order of magnitude higher than the typical frequency (~1 Hz) of Earth's ionospheric Alfvén resonator [*Lysak*, 1993], we cannot rule out this possible driver. A short ionospheric scale height would result a high reoccurrence rate. Here, we suggest multiple Alfvénic disturbances in the magnetotail as another possible driver for the reoccurrence of discrete short-bursts. *Su et al.* [2007] demonstrated that multiple shell electron distributions were generated by multiple Alfvén wave pulses with equal time spacing. Because multiple shells (or rings) were found in each of the eight events, multiple initial wave pulses are likely to be the source. Each discrete short-burst radiation is then generated when unstable distributions due to each waves pulse passed through regions with conditions matching the maser instability.

[30] We found that the spectral power density of short burst emissions is one or two orders weaker than that of typical AKRs. If AKRs and short-bursts were present simultaneously, it would be difficult to distinguish weak S-bursts from strong AKR signals. AKRs are observed to be associated with "inverted-V" electron signatures in the upward current region. On the basis of our extensive study, the upward current region is often adjacent to the Alfvénic acceleration region. The strong AKR signals from the adjacent upward current region might overpower weak short-bursts in the Alfvénic region. This may be one of the reasons why the occurrence rate of short-burst events is very low. Eight events in 3 years represent the minimum occurrence rate.

[31] Another likely reason for the low occurrence rate is the plasma condition in the emission source region. At Jupiter, the condition for the weakly relativistic cyclotron maser instability $\omega_{pe}/\omega_{ce} \ll 1$ is easily satisfied above a few thousand kilometers up to ~4 R_J due to Jupiter's strong magnetic field [*Ergun et al.*, 2006]. This explains the higher occurrence rate of S-bursts at Jupiter. The low occurrence rate at Earth was anticipated by *Su et al.* [2007].

[32] Based on a single event study, *Su et al.* [2007] suggested that single and multiple shell distributions, as well as electron conics (rings), generated by propagating Alfvén waves are the sources of short-bursts. Our results strongly support this idea. Recently, we performed simulations of the electron cyclotron maser instability using an electromagnetic particle-in-cell code [*Pritchett et al.*, 1999, 2002]. It was found that the observed electron distributions are good candidates for triggering the maser instability. An example of this is presented in Figure 5. The initial unstable electron distribution (Figures 5a and 5b) provides the energy to excite electromagnetic waves and fills the loss cone until the gradient is diminished (Figures 5c and 5d). The initial distribution in Figure 5a resembles the ring distribution in Figure 4d, while the end distribution in Figure 5c is similar to the observed distribution shown in the dashed rectangular box in Figure 4h. A complete report on our simulation results will be featured in a separate paper. Electron distributions from FAST observations reported here will serve as initial input parameters for future maser simulation studies.

[33] Although the plasma conditions for triggering the maser instabilities are the same for the common AKRs and the short-burst radiations, the source mechanisms of the two are different. While AKRs are generated by horseshoe distributions in the auroral density cavity between two parallel potential drops in the quasi-steady upward current region, the short bursts can be generated by partial shells, conics, or rings due to the dynamics of Alfvén waves. The area of positive phase-space density gradient in providing free energy for short-burst radiations is smaller than that of the horseshoes for AKRs. This may be the reason why the observed power of short-burst is smaller than that of common AKRs. In addition, in the quasi-steady upward current region, there may be a continuous supply of unstable distributions due to a quasi-steady parallel electric field. However, in the dynamic Alfvénic region, the parallel electric field varies within the inertial Alfvén wave period. This may be able to explain why Alfvénic associated

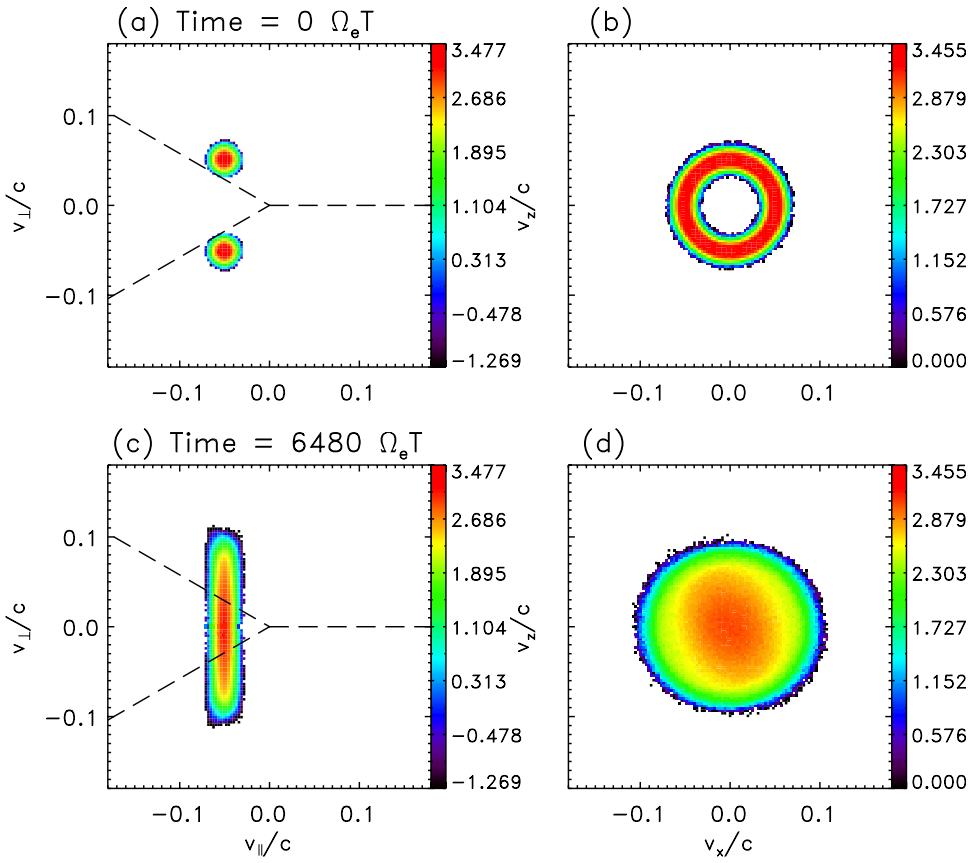

Figure 5. Electron distributions from the simulation of the electron cyclotron maser instability. (a) The initial electron distribution. The vertical and horizontal axes represent the perpendicular and parallel velocities in the unit of the light speed, where the negative $V_{\|}$ (=V_y) is the direction away from the ionosphere. The dashed lines in the upward direction indicate the loss cone. (b) The initial electron distribution plotted in the perpendicular velocity plane (V_x, V_z). The beam signature in Figure 5a is a ring distribution in the perpendicular velocity plane (Figure 5b). (c) The end distribution where the phase space gradient at the loss cone boundary is diminished. (d) The end distribution in the perpendicular velocity plane.

emissions are discrete short bursts rather than the continuous spectrum observed in typical AKRs.

[34] **Acknowledgments.** The authors would like to thank the FAST team for providing the FAST data and the data analysis tool. The authors thank Fran Bagenal, Philip Zarka, and Sebastian Hess for helpful discussions. The first author thanks Don Gurnett for providing useful references and Ron Caton for proofreading the manuscript. This research was supported by the NASA grant NNG05GM99G and the NSF/CAREER award ATM-0544656 to UT Arlington.

[35] Amitava Bhattacharjee thanks Jan Hanasz and another reviewer for their assistance in evaluating this paper.

References

Baart, E. E., C. H. Barrow, and R. T. Lee (1966), Millisecond radio pulses from Jupiter, *Nature*, *211*, 805.

Benediktov, E. A., G. G. Getmantsev, Y. A. Sazonov, and A. F. Tarojov (1965), Preliminary results of measurements of the intensity of distributed extra-terrestrial radio frequency emission at 725 and 1525 kHz, *Kosm. Issled.*, *3*, 614.

Benson, R. F., and W. Calvert (1979), ISIS 1 observations at the source of auroral kilometric radiation, *Geophys. Res. Lett.*, *6*, 479.

Benson, R. F., M. M. Mellott, R. L. Huff, and D. A. Gurnett (1988), Ordinary mode auroral kilometric radiation fine structure observed by DE 1, *J. Geophys. Res.*, *93*, 7515.

Calvert, W., Y. Leblanc, and G. R. A. Ellis (1988), Natural radio lasing at Jupiter, *Astrophys. J.*, *335*, 976.

Carr, T. D., and F. Reyes (1999), Microstructures of Jovian decametric S bursts, *J. Geophys. Res.*, *104*, 25,127.

Carr, T. D., M. D. Desch, and J. K. Alexander (1983), Phenomenology of magnetospheric radio emissions, in *Physics of the Jovian Magnetosphere*, edited by A. J. Dessler, 226 pp., Cambridge Univ. Press, New York.

Chaston, C. C., J. W. Bonnell, C. W. Carlson, M. Berthomier, L. M. Peticolas, I. Roth, J. P. McFadden, R. E. Ergun, and R. J. Strangeway (2002a), Electron acceleration in the ionospheric Alfvén resonator, *J. Geophys. Res.*, *107*(A11), 1413, doi:10.1029/2002JA009272.

Chaston, C. C., J. W. Bonnell, L. M. Peticolas, C. W. Carlson, J. P. McFadden, and R. E. Ergun (2002b), Driven Alfvén waves and electron acceleration: A FAST case study, *Geophys. Res. Lett.*, *29*(11), 1535, doi:10.1029/2001GL013842.

Delory, G. T., R. E. Ergun, C. W. Carlson, L. Muschietti, C. C. Chaston, W. Peria, J. P. McFadden, and R. Strangeway (1998), FAST observations of electron distributions within AKR source regions, *Geophys. Res. Lett.*, *25*, 2069.

Desch, M. D., R. S. Flagg, and J. May (1978), Jovian S-burst observations at 32 MHz, *Nature*, *272*, 38.

Dulk, G. A., A. Lecacheux, and Y. Leblanc (1992), The complete polarization state of a storm of millisecond bursts from Jupiter, *Astron. Astrophys.*, *253*, 292.

Ellis, G. R. A. (1980), The source of Jupiter S-bursts, *Nature*, *293*, 48.

Ergun, R. E., et al. (1998), FAST satellite wave observations in the AKR source region, *Geophys. Res. Lett.*, *25*, 2061.

Ergun, R. E., C. W. Carlson, J. P. McFadden, G. T. Delory, R. J. Strangeway, and P. L. Pritchett (2000), Electron-cyclotron maser driven by charged-particle acceleration from magnetic field-aligned electric fields, *Astrophys. J.*, *538*, 456.

Ergun, R. E., et al. (2001), The Fast satellite fields instruments, *Space Sci. Rev.*, *98*, 67.

Ergun, R. E., Y.-J. Su, L. A. Andersson, F. Bagenal, P. A. Delamere, R. L. Lysak, and R. J. Strangeway (2006), S-Bursts and the Jupiter ionospheric Alfvén resonator, *J. Geophys. Res.*, *111*, A06212, doi:10.1029/2005JA011253.

Gallet, R. M. (1961), Radio observations of Jupiter II, in *Planets and Satellites*, edited by G. P. Kuiper, 500 pp., Univ. of Chicago Press, Chicago.

Genova, F., and W. Calvert (1988), The source location of Jovian millisecond radio bursts with respect to Jupiter's magnetic field, *J. Geophys. Res.*, *93*, 979.

Gurnett, D. A. (1974), The Earth as a radio source: Terrestrial kilometric radiation, *J. Geophys. Res.*, *79*, 4227.

Gurnett, D. A., and R. R. Anderson (1981), The kilometric radio emission spectrum: Relationship to auroral acceleration processes, in *Physics of Auroral Arc Formation*, *Geophys. Monogr. Ser.*, vol. 25, edited by S.-I. Akasofu and J. R. Kan, 341 pp., AGU, Washington, D. C.

Gurnett, D. A., and J. L. Green (1978), On the polarization and origin of auroral kilometric radiation, *J. Geophys. Res.*, *77*, 172.

Gurnett, D. A., R. R. Anderson, F. L. Scarf, R. W. Fredericks, and E. J. Smith (1979), Initial results from the ISEE 1 and 2 plasma wave investigation, *Space Sci. Rev.*, *23*, 103.

Hewitt, R. G., D. B. Melrose, and K. G. Ronnmark (1981), A cyclotron theory for the beaming pattern of Jupiter's decametric radio emission, *Proc. Astron. Soc. Aust.*, *4*, 221.

Hewitt, R. G., D. B. Melrose, and K. G. Ronnmark (1982), The loss-cone driven electron-cyclotron maser, *Aus. J. Phys.*, *35*, 447.

Hilgers, A. (1992), The auroral radiating plasma cavities, *Geophys. Res. Lett.*, *19*, 237.

Kaiser, M. L., J. K. Alexander, A. C. Riddle, J. B. Pearce, and J. W. Warwick (1978), Direct measurements of the polarization of terrestrial kilometric radiation from Voyagers 1 and 2, *Geophys. Res. Lett.*, *5*, 857.

Keiling, A., J. R. Wygant, C. Cattell, M. Johnson, M. Temerin, F. S. Mozer, C. A. Kletzing, J. Scudder, and C. T. Russell (2001), Properties of large electric fields in the plasma sheet at $4-7\ R_E$ measured with Polar, *J. Geophys. Res.*, *106*, 5779.

Keiling, A., J. R. Wygant, C. A. Cattell, F. S. Mozer, and C. T. Russell (2003), The global morphology of wave Poynting flux: Powering the aurora, *Science*, *299*, 383.

Kraus, J. D. (1956), Some observations of the impulsive radio signals from Jupiter, *Astron. J.*, *61*, 182.

Kumamoto, A., and H. Oya (1998), Asymmetry of occurrence frequency and intensity of AKR between summer polar region and winter polar region sources, *Geophys. Res. Lett.*, *25*, 2369.

Kurth, W. S., M. M. Baumback, and D. A. Gurnett (1975), Direction finding measurements of auroral kilometric radiation, *J. Geophys. Res.*, *80*, 2764.

Leblanc, Y., F. Genova, and J. de La Noë (1980), The Jovian S-bursts, *Astron. Astrophys.*, *86*, 342.

Lecacheux, A., N. Meyer-Vernet, and G. Daigne (1981), Jupiter's decametric radio emission: A nice problem of optics, *Astron. Astrophys.*, *94*, L9.

Louarn, P. (1992), Auroral planetary radio emissions, theoretical aspects, *Adv. Space Res.*, *12*, 121.

Louarn, P., A. Roux, H. de Feraudy, D. Le Queau, M. Andre, and L. Matson (1990), Trapped electrons as a free energy source for the auroral kilometric radiation, *J. Geophys. Res.*, *95*, 5983.

Lysak, R. L. (1993), Generalized model of the ionospheric Alfvén resonator, in *Auroral Plasma Dynamics*, *Geophys. Monogr.*, vol. 80, edited by R. Lysak, 121 pp., AGU, Washington, D. C.

Lysak, R. L., and Y. Song (2003), Nonlocal kinetic theory of Alfvén waves on dipolar field lines, *J. Geophys. Res.*, *108*(A8), 1327, doi:10.1029/2003JA009859.

Melrose, D. B. (1976), An interpretation of Jupiter's decametric radiation and the kilometric radiation as direct amplified gyroemission, *Astrophys. J.*, *207*, 651.

Melrose, D. B. (1986), A phase-bunching mechanism for fine structure in auroral kilometric radiation and Jovian decametric radiation, *J. Geophys. Res.*, *91*, 7970.

Melrose, D. B., and G. A. Dulk (1982), Electron-cyclotron masers as the source of certain solar and stellar radio bursts, *Astrophys. J.*, *259*, 844.

Menietti, J. D., H. K. Wong, W. S. Kurth, D. A. Gurnett, L. J. Granroth, and J. B. Groene (1996), Discrete, stimulated auroral kilometric radiation observed in the Galileo and DE1 wideband data, *J. Geophys. Res.*, *101*, 10,673.

Menietti, J. D., H. K. Wong, W. S. Kurth, D. A. Gurnett, L. J. Granroth, and J. B. Groene (1997), Possible stimulated AKR observed in Galileo, DE-1, and Polar wideband data, in *Planetary Radio Emissions IV*, edited by H. O. Rucker, S. J. Bauer, and A. Lecacheux, Austrian Acad. of Sci. Press, Vienna, Austria.

Menietti, J. D., A. M. Persoon, J. S. Pickett, and D. A. Gurnett (2000), Statistical study of auroral kilometric radiation fine structure striations observed by Polar, *J. Geophys. Res.*, *105*, 18,857.

Morioka, A., H. Oya, and S. Miyatake (1981), Terrestrial kilometric radiation observed by satellite JIKKIKEN (EXOS-B), *J. Geomagn. Geoelectr.*, *33*, 37.

Pritchett, P. L., and R. M. Winglee (1989), Generation and propagation of kilometric radiation in the auroral plasma cavity, *J. Geophys. Res.*, *94*, 129.

Pritchett, P. L., R. J. Strangeway, C. W. Carlson, R. E. Ergun, J. P. McFadden, and G. T. Delory (1999), Free energy sources and frequency bandwidth for the auroral kilometric radiation, *J. Geophys. Res.*, *104*, 10,317.

Pritchett, P. L., R. J. Strangeway, R. E. Ergun, and C. W. Carlson (2002), Generation and propagation of cyclotron maser emissions in the finite AKR source cavity, *J. Geophys. Res.*, *107*(A12), 1437, doi:10.1029/2002JA009403.

Queinnee, J., and P. Zarka (2001), Flux, power, energy, and polarization of Jovian S-bursts, *Planet. Space Sci.*, *49*, 365.

Riihimaa, J. J. (1977), S-bursts in Jupiter's decametric radio spectra, *Astrophys. Space Sci.*, *51*, 363.

Ryabov, V. B., B. P. Ryabov, D. M. Vavriv, P. Zarka, R. Kozhin, V. V. Vinogradov, and V. A. Shevchenko (2007), Jupiter S-bursts: Narrowband origin of microsecond subpulses, *J. Geophys. Res.*, *112*, A09206, doi:10.1029/2007JA012607.

Shawhan, S. D., and D. A. Gurnett (1982), Polarization measurements of auroral kilometric radiation by Dynamics Explorer-1, *Geophys. Res. Lett.*, *9*, 913.

Strangeway, R., et al. (1998), FAST observations of VLF waves in the auroral zone: Evidence of very low plasma densities, *Geophys. Res. Lett.*, *25*, 2065.

Su, Y.-J., R. E. Ergun, W. K. Peterson, T. G. Onsager, R. Pfaff, C. W. Carlson, and R. J. Strangeway (2001), Fast Auroral Snapshot observations of cusp electron and ion structures, *J. Geophys. Res.*, *106*, 25,595.

Su, Y.-J., S. T. Jones, R. E. Ergun, F. Bagenal, S. E. Parker, P. A. Delamere, and R. L. Lysak (2006), Io-Jupiter interaction: Alfvén wave propagation and ionospheric Alfvén resonator, *J. Geophys. Res.*, *111*, A06211, doi:10.1029/2005JA011252.

Su, Y.-J., R. E. Ergun, S. T. Jones, R. J. Strangeway, C. C. Chaston, S. E. Parker, and J. L. Horwitz (2007), Generation of short-burst radiation through Alfvénic acceleration of auroral electrons, *J. Geophys. Res.*, *112*, A06209, doi:10.1029/2006JA012131.

Winglee, R. M., G. A. Dulk, and P. L. Pritchett (1988), Fine structure of microwave spike bursts and associated cross-field transport, *Astrophys. J.*, *332*, 466.

Winglee, R. M., J. D. Menietti, and H. K. Wong (1992), Numerical simulations of bursty radio emissions from planetary magnetosphere, *J. Geophys. Res.*, *97*, 17,131.

Wu, C. S., and L. C. Lee (1979), A theory of the terrestrial kilometric radiation, *Astrophys. J.*, *230*, 621.

Wygant, J. R., et al. (2000), Polar spacecraft based comparisons of intense electric fields and Poynting flux near and within the plasma sheet-tail lobe boundary to UVI images: An energy source for the aurora, *J. Geophys. Res.*, *105*, 18,675.

Zarka, P. (1992), The auroral radio emissions from planetary magnetospheres: What do we know, what don't we know, what do we learn from them?, *Adv. Space Res.*, *12*, 115.

Zarka, P. (1998), Auroral radio emissions at the outer planets: Observations and theories, *J. Geophy. Res.*, *103*, 20,159.

Zarka, P. (2004), Radio and plasma wave at the outer planet, *Adv. Space Res.*, *33*, 2045.

Zarka, P., T. Farges, B. P. Ryabov, M. Abada-Simon, and L. Denis (1996), A scenario for Jovian S-bursts, *Geophys. Res. Lett.*, *23*, 125.

C. W. Carlson, Space Sciences Laboratory, University of California, Berkeley, 7 Gauss Way #7450, Berkeley, CA 94720, USA. (cwc@ssl.berkeley.edu)

R. E. Ergun, Laboratory for Atmospheric and Space Physics, University of Colorado, Boulder, CO 80303, USA. (ree@fast.colorado.edu)

L. Ma and Y.-J. Su, Physics Department, University of Texas at Arlington, 502 Yates, Science Hall Room 108, Box 19059, Arlington, TX 76019, USA. (yijiun@uta.edu)

P. L. Pritchett, Department of Physics and Astronomy, University of California, 405 Hilgard Avenue, Los Angeles, CA 90095, USA. (pritchet@physics.ucla.edu)